International Journal of Thermofluid Science and Technology (2022)
Volume 9, Issue 3, Paper No. 090305
https://doi.org/10.36963/IJTST.2022090305
Research Article

Study of flow fluctuation in the thermal bubble pump tube

Ali Benhmidene*, Rabeb Jemaii, Khaoula Hidouri, Bechir Chaouachi

Depatement of Chemical Engineering Process, The School of Engineering of Gabès, Gabès University, Zrig, Gabès, Tunisia

ARTICLE INFO

Received: 12 Jan. 2022;
Received in revised form:
16 Feb. 2022;
Accepted: 28 Mar. 2022;
Published online:
30 Mar. 2022

Keywords:
Turbine
Empirical model
Mass flow rate
Isentropic Efficiency
Mean value model

ABSTRACT

In the present work, we were interested in the study of the oscillatory phenomenon of ammonia-water two-phase flow inside the bubble pump of absorption-diffusion refrigerators. In fact, flow instability can reduce the efficiency of the bubble pump. The simulation of two-phase flow in the bubble pump is conducted by using the drift flow model. Balance equations of the drift flow model and their closure relationships, as well as the numerical method, were developed. The numerical resolution allowed defining the void fraction, the liquid and vapor velocities, the pressure, and the mixing enthalpy against time. The effect of heat flux received by the bubble pump is simulated in the transitional regime. Simulated results of the vapor, liquid, and mass velocities show a flow fluctuation at the beginning of the operation. The duration of the fluctuation increase from 6s to 12s by reducing the heat flux from 5 to 2kW/m².The void fraction profile makes it possible to distinguish that the slug and churn regimes are those which dominate the pump's operating regime for a heat flux of 2 and 3 kW/m². The pumping action is influenced by the heat flux. A maximum of 10kW/m² value of heat flux is defined for an obtained minimum of the pumping action.

1. Introduction

Absorption-diffusion refrigerators (DAR) have the advantage that they operate at a uniform pressure and therefore no moving parts. The absence of any mechanical work input makes for a quiet and very reliable machine suitable for hotel rooms, offices, and camping cars [1].

The bubble pump is the key part of DAR machine, as it is responsible, in the absence of a mechanical pump, for circulating the fluid and desorbing the refrigerant from the mixture. It consists of a vertical heated tube containing a boiling two-phase mixture. The efficiency of the bubble pump has a direct and significant influence on the efficiency of the absorption-diffusion refrigerators. Subsequently, an oscillatory phenomenon may occur due to this flow along the tube. Similarly, heating process can be a factor in inducing instability.

*Corresponding e-mail: ali.benhmidene@gmail.com(Ali Benhmidene)

Nomenclature

A	tube section, m^2	t	time, s
C_o	distribution coefficient	x	vapor quality
$C_{1,2}$	coefficients of drift velocity	X	mass fraction
Cp	thermal capacity, J/kg.°C	*Greek symbols*	
D	tube diameter, m	α	void fraction
f	friction factor	ρ	density, kg/m^3
g	presenter acceleration, m/s^2	Γ	vapor generation rate, $kg/m^3.s$
G	mass velocity, $kg/m^2.s$	μ	dynamic viscosity, Pa.s
H	specific enthalpy, J/kg	λ	thermal conductivity, W/m.K
h	heat transfer coefficient, $W/m^2.K$	σ	surface tension, N/m
h_{fg}	vaporization enthalpy, J/kg	*Subscripts*	
J	volume flow, m^3/s^1	f	friction
P	Pressure, Pa	m	mixing
Pr	Prendtl number	OSV	onset significant void
q	heat flux, W/m^2	tp	two phase
Re	Reynolds number	sp	single phase
T	temperature, K	w	wall
Vjg	drift velocity, m/s		

Historically, the study of two-phase flows instabilities was started with the pioneering article by Ledinegg [2]. Since 1960, the development of high power density industrial boilers and boiling water reactors draws the attention of many researchers to the phenomenon occurring in two-phase flow systems [3 – 6].During these years, several experimental studies have interesting of boiling flow in pipelines such as the one described by Yadigaroglu [7]. Through the development of numerical analysis tools, several authors studied the main mechanisms of instability in the decade of 1960s [8 – 11]. During the 1970s and early 1980s, several analytical works contributed to the understanding of thermal and hydraulic instabilities such as Fukuda and Kobori [12]. The study of thermal-hydraulic instabilities is linked to the analysis of accidents in nuclear reactors; the rapid development of calculation tools allows the transient phenomenon in nuclear reactors to be studied.

Today, the different scenarios where phenomena fluctuation can occur in the nuclear industry are understood. Mayinger [13] noted that most of the research today on thermo-hydraulic instabilities belongs to the field of nuclear safety. Also, for the oil and chemical industries, the understanding of theinstability phenomenon of two-phase flows occurring in its components is still limited. Over the last 50 years, several works have reported the appearance of the flow instability in the heating components such as heat exchangers, heaters, economizers, steam generators, condensers, oil well components, thermosiphons…[14,15].

However, there is very little data or research describing the oscillatory phenomenon in absorption-diffusion machines. Most of the work carried out does not deal in detail with the fluid behavior in this compound of the single-pressure machines, and they are limited to the writing of overall input-output balances [16, 17]. Also, not all authors attempt to explain the causes or the types of presented oscillations. To understand the oscillatory phenomenon in boiling heat exchangers, several experimental and theoretical studies on

the instabilities of two-phase flow in circular channels have been published [18]. Most of the studies found in the literature have been carried out on parallel or single channels, but with non-uniform heat density [19-21]. The design of the bubble pump presents a challenge to the designer because all the risks of degradation, breakage and leakage of the bubble pumptube must be taken into consideration. For this, a theoretical and experimental study of the oscillation phenomenon that occurs in the bubble pump is important. This can be carried out by simulating two-phase flows [22-24].

Various models for simulating two-phase flow in the heated tubes have been developed. The three main models used are the homogeneous, drift, and two-fluid model. The homogeneous model is the simplest model which assumes a thermal and hydrodynamic equilibrium between phases. The two-fluid model is the most general formulation for two-phase flow modeling where it treats each phase or component as a separate fluid with its own set of equilibrium equations [25-27]. The drift model is the most commonly used for describing and simulating transient phenomena and characterizing two-phase flow in up-flow and boiling flow systems [28]. It assumes the existence of a relative velocity between phases. The fluid properties are represented by the properties of the mixture, making drift flow formulation simpler than two-fluid formulation [29].

The present work is a simulation of the influence of heat flux on the flow fluctuations in the bubble pump tube. To aim our goal, two-phase flow is modeling by used the drift flow model. The main parameters studied are liquid, vapor, and mass velocities. In addition, void fraction and pumping ratio are simulated too.

2. Mathematical Formulation

The drift-flux model consists of four equations: one conservation of mass for the mixture, one conservation of mass for the gas phase, one conservation of momentum for the mixture, and one conservation of energy for the mixture. This approach is usually preferred over the two-fluid model due to its simplicity and flexibility. It is important to note that the drift-flux model is better suited for cases when there is strong coupling and local relative motion between the liquid and gas phases, which is typically the case for bubbly and slug flow regimes [29]. For stratified or annular flow regimes, the two-fluid model approach provides better predictions.

The mean parameters of drift flux model are the two-phase mixture velocity (Vm), the distribution parameter (C_0), and the drift velocity (Vjg).

The distribution parameter (C_0) accounts for the distribution of the gas phase across the pipe cross section and acts as a correction factor for the assumption of no local slippage between the liquid and gas phases. The drift velocity (Vjg) represents the cross sectional void fraction weighted average of the local relative velocity of the gas phase with respect to the two-phase mixture velocity at the pipe volume center.

As suggested by Zuber and Findlay [30], the value of C_0 should be:

− Dependent on the flow and void fraction profiles,

− In the range from about 1.0 to 1.5 when the void fraction close to the pipe wall is smaller than that at the pipe center,

− In the range less than 1.0 when the void fraction close to the wall is greater than that at the pipe center,

− Constant if the flow is fully developed and has constant profiles.

2.1 Drift model equations

The drift flow model was used for the two-phase flow region in the bubble pump. Their conservation equations of mass, momentum, and energy are formulated for the fowling assumptions:

- Transient regime
- Kinetic and potential energy are negligible
- One-dimensional flow
- Heat input is supplied along the tube
- Same pressure for liquid and vapour phases

Mixture continuity

$$\frac{\partial \rho_m}{\partial t} + \frac{\partial}{\partial z}(\rho_m . V_m) = 0 \qquad (1)$$

- Gas continuity

$$\frac{\partial\left(\alpha_g.\rho_g\right)}{\partial t}+\frac{\partial}{\partial z}\left(\alpha_g\rho_g V_m\right)=\Gamma_g-\frac{\partial}{\partial z}\left[\frac{\alpha_g\rho_l\rho_g}{\rho_m}\overline{V}_{gj}\right] \quad (2)$$

- Mixture momentum

$$\frac{\partial(\rho_m.V_m)}{\partial t}=-\frac{\partial}{\partial z}(\rho_m.V_m^2)-\frac{\partial P}{\partial z}-\rho_m g-\frac{f_m}{D_h}\rho_m V_m^2-\frac{\partial}{\partial z}\left[\frac{\alpha\rho_G\rho_L}{(1-\alpha)\rho_m}\overline{V}_{gj}^2\right] \quad (3)$$

- Mixture energy

$$\frac{\partial}{\partial t}(\rho_m h_m)+\frac{\partial}{\partial z}(\rho_m h_m V_m)=\frac{q_w\Omega}{A} \quad (4)$$

2.2 Drift velocity and distribution coefficient

From the balance of buoyancy and drag forces, the average drift velocity of the dispersed phase noted $\overline{V_{gj}}$ is correlated as a function of void fraction, liquid and vapour densities. These parameters depend on the operating conditions as well as the flow regimes. In addition, the average drift velocity takes into account the diffusion effects. It is expressed by Eq. (5) [31, 32]:

$$\overline{V}_{gj}=\frac{\rho_m(v_{gj}+(C_0-1)V_m)}{\rho_m-(C_0-1)\alpha\,(\rho_l-\rho_g)} \quad (5)$$

Where V_m ,v_{gj} are respectively the velocity of the liquid-vapor mixture and the local drift velocity. Ishii [31-33] has developed the equation of distribution parameter C_0 for vertical boiling flow as a function of void fraction. The following equation of C_0 describes the effect of nucleated bubbles on the void distribution.

$$C_0=1.2-0.2\sqrt{\frac{\rho_g}{\rho_l}}\{1-exp(-18\alpha)\} \quad (6)$$

Also, Ishii [33] has took into account the interfacial geometry, the body force field, the shear stresses and the interfacial momentum transfer to define the equation of local drift velocity. The different correlations local drift velocity for different regimes are defined as follows:

- Bubbly flow

$$v_{gj}=\sqrt{2\left(\frac{g\sigma\Delta\rho}{\rho_l^2}\right)^{1/4}}(1-\alpha)^{1.75} \text{ for } \mu_l>>\mu_g \quad (7)$$

- Slug flow

$$v_{gj}=0.35\left(\frac{gD\Delta\rho}{\rho_l}\right)^{1/2} \quad (8)$$

- Churn flow

$$v_{gj}=\sqrt{2\left(\frac{g\sigma\Delta\rho}{\rho_l^2}\right)^{1/4}} \quad (9)$$

- Annular flow

The kinematic equation of the mean dispersed phase drift velocity for a two-phase annular flow was developed taking into account macroscopic effects. Ishii [33] determined the expression of this velocity for the vapor phase as follows

$$\overline{V}_{gj}=\frac{1-\alpha}{\langle\alpha\rangle+\left\{\frac{1+75(1-\alpha)}{\sqrt{\alpha}}\frac{\rho_g}{\rho_l}\right\}^{\frac{1}{2}}}\left\{\langle j\rangle+\sqrt{\frac{gd\Delta\rho(1-\alpha)}{0.015\,\rho_l}}\right\} \quad (10)$$

Where $\langle j\rangle$ represents the volume flow. It is defined as follows [32]:

$$\langle j\rangle=(1-\alpha)v_l+\alpha\,v_g \quad (11)$$

Liquid and vapor velocities are defined by [31, 32]:

$$v_g=V_m+\frac{\rho_l}{\rho_m}\overline{V}_{gj} \quad (12)$$

$$v_l=V_m-\frac{\alpha\rho_g}{(1-\alpha)\rho_m}\overline{V}_{gj} \quad (13)$$

Mass velocity is a function of v_g and v_l, it's given by:

$$G=\alpha\rho_g v_g+(1-\alpha)\rho_l v_l \quad (14)$$

Replacing v_g and $v_l$by their in expression in Eq. (11), $\langle j\rangle$ can be expressed as follows [32]:

$$\langle j\rangle=V_m+\frac{\alpha(\rho_l-\rho_g)}{\rho_m}\overline{V}_{gj} \quad (15)$$

Combining Eqs (10) and (15) gives a new expression for $\overline{V}_{gj}$[32]

$$\overline{V}_{gj}=\frac{C_1v_m+C_1C_2}{1-C_1\frac{\alpha(\rho_l-\rho_g)}{\rho_m}} \quad (16)$$

Where C_1 and C_2 are two coefficients defined as follows [32]:

$$C_1=\frac{(1-\alpha)}{\alpha+4\sqrt{\rho_g/\rho_l}} \quad (17)$$

$$C_2=\sqrt{\frac{gd\Delta\rho\,(1-\alpha)}{0.015\,\rho_l}} \quad (18)$$

2.3 Friction pressure drop

Using various methods, the friction pressure drop for two-phase flow can be calculated based on the separate flow theory. The Lockhart and Martinelli correlation was the first to represent this coefficient, but it is

used for system pressures close to atmospheric pressure and for fluids other than water [34]. The Müller-Steinhagen and Heck [32, 35] correlation gave accurate and better results for simple and binary fluids. Therefore, we have chosen it in our work. It is an empirical interpolation between the frictional pressure drop of liquid flow f_{lo} and vapour flow f_{go}. The expression of two-phase friction is given by:

$$f_m = Bx^3 + F(1-x)^{\frac{1}{3}} \quad (19)$$

$$F = A + 2(B - A)x \quad (20)$$

$$A = f_{lo}\frac{\rho}{\rho_l} \quad (21)$$

$$B = f_{go}\frac{\rho}{\rho_g} \quad (22)$$

Where the expression of vapor quality is:

$$x = \frac{1}{1 + \frac{(1-\alpha)}{\alpha}\cdot\frac{\rho_l}{\rho_g}\cdot\frac{v_l}{v_g}} \quad (23)$$

The phase friction liquid f_{lo} is given in function of Reynolds number of liquid phase:

$$f_{Lo} = \begin{cases} \frac{16}{Re_{lo}} for Re_{lo} = \frac{GD}{\mu_l} \le 2000 \\ 0.0079 Re_{lo}^{-0.25} for Re_{lo} = \frac{GD}{\mu_l} > 2000 \end{cases} \quad (24)$$

Similarly the phase friction of vapor alone is expression in function of Reynolds number too:

$$f_{go}\begin{cases} \frac{16}{Re_{go}} for Re_{go} = \frac{GD}{\mu_l} \le 2000 \\ 0.0079 Re_{go}^{-0.25} for Re_{go} = \frac{GD}{\mu_g} > 2000 \end{cases} \quad (25)$$

2.4 Vapor generation rate

The vapor generation rate is given as follows [36]:

$$\Gamma_g = \frac{q_E}{(h_{fg} + Cp_l \Delta T_{sat})}\frac{4}{D} \quad (26)$$

The heat flux due to evaporation q_E is given by Eq. (27) [37]:

$$q_E = C_2\left(q_w - C_1\, h_{sp}\ (T_w - T_l)\right) \quad (27)$$

Where:

$$C_1 = 1 - \frac{\pi}{16}\frac{\alpha}{\alpha_{osv}} \quad for\ \alpha \le \frac{16.\alpha_{osv}}{\pi} \quad (28)$$

$$C_1 = 0 \quad for\ \alpha > \frac{16.\alpha_{osv}}{\pi} \quad (29)$$

$$C_2 = \left(\frac{T_w - T_{sat}}{T_w - T_l}\right)^2 \quad (30)$$

The Dittus-Boelter correlation [38] of single phase heat transfer h_{sp} given by Eq. (31) is used in our simulation.

$$h_{sp} = 0.023\frac{\lambda_l}{D} Re_l^{0.8} Pr_l^{0.4} \quad (31)$$

Where: Reynolds number of the liquid phase Re_l is given by:

$$Re_l = \frac{GD(1-x)}{\mu_l} \quad (32)$$

The Prandtl number of the liquid phase Pr_l is expressed as follows:

$$Pr_l = \frac{Cp_l \mu_l}{\lambda_l} \quad (33)$$

2.5 Resolution method

To obtain a system of ordinary differential equations that is easier to solve, the following changes of variables are made:

$$u_1 = \rho_m \quad (34)$$

$$u_2 = \alpha\rho_g \quad (35)$$

$$u_3 = \rho_m V_m \quad (36)$$

$$u_4 = \rho_m h_m \quad (37)$$

The system of ordinary equation has the following general form:

$$\frac{\partial U}{\partial t} = Q(U) + \frac{\Delta F(U)}{L} \quad (38)$$

Where

$$U = \begin{bmatrix} u_1 \\ u_2 \\ u_3 \\ u_4 \end{bmatrix} \quad (39)$$

$$Q = \begin{bmatrix} 0 \\ \Gamma_g \\ \rho_m\, g + \frac{f_m}{D_h}\rho_m V_m^2 \\ \frac{q f_h}{A_c} \end{bmatrix} \quad (40)$$

$$F = \begin{bmatrix} -(\rho_m . V_m) \\ -\left(\alpha\rho_g V_m + \frac{\alpha\rho_G\rho_L}{(1-\alpha)\rho_m}\overline{V}_{gj}^2\right) \\ -\left(\rho_m . V_m^2 + \frac{\alpha\rho_G\rho_L}{(1-\alpha)\rho_m}\overline{V}_{gj}^2\right) \\ -(\rho_m h_m V_m) \end{bmatrix} \quad (41)$$

The system of ordinary differential equations (ODE) of variables u_1, u_2, u_3 and u_4 is solved by adopting the Runge Kutta fourth order method using Matlab 13 software.

Flow parameters are deduced from the variables of the system of ordinary differential equations as follows:

$$\alpha = u_2/\rho_g \quad (42)$$

$$V_m = u_3/u_1 \quad (43)$$

$$H_m = u_4/u_1 \quad (44)$$

2.6 Initial and boundary conditions

For the Drift model, the bubble pump tube was initially filly with ammoia-water mixing liquid with a simple trace of vapor.

So the initial and the boundary conditions are specified as follows:

- Ammonia mass fraction in the mixing x(0,0) = 0.6
- Void fraction $\alpha(0, 0) = 10^{-3}$ [39]
- Pressure P(0, 0) = 13 bar
- Vapor velocity vg(z, 0) = 0 m/s, liquid velocity $V_L(z,0)$ has the same value of the mixing velocity $V_m(z,0)$ equal to the ratio of mass velocity G by mixing density in the entrance ($G/\rho(0,t)$);
- The inlet temperature is the saturated flow temperature at pressure in the inlet: T(0,0) = 59.28 °C
- Liquid enthalpy in the inlet is equal to mixing enthalpy : $H(0,t) = H_m(0,t)$

The physical proprieties at the inlet are of the saturated mixing at the entrance to the bubble pump tube.

2.7 Physicochemical properties

The inlet saturated pressure is given by Bourseau and Bugarel correlation [40] as fellow:

$$\log P = A - \frac{B}{T} \quad (45)$$

$$A = 7.44 - 1.767X + 0.9823X^2 + 0.3627X^3 \quad (46)$$

$$B = 2013.8 - 2155.7X + 1540.9X^2 - 1947X^3 \quad (47)$$

The density of the liquid is calculated using the correlation of Tiliner-Roth and Friend [41] (see Appendix 1). The correlation of Pátek and Klomfar [42] in Appendix 2 was used to calculate the enthalpy of the mixture at the inlet.

3. Results and Discussion

In the present study, we interest to simulate an ammonia-water two-phase flow in the bubble pump heating along its tube. In order to study the fluctuation phenomenon in the bubble pump, we focused our study on the flow parameters as a function of the time. The studied parameters are the liquid, vapor and mass velocities. In addition, the pumping ratio, and void fraction are studied too. Our study interests especially on the influence of the heat flux received by the bubble pump on the two-phase flow behavior. The simulation results are presented using the operating conditions given in Table1.

3.1. Model validation

In order to validate our simulation results, we compared the simulated void fraction with others proposed by different authors (Smith [43], Lockhart and Martinelli [44], Zivi [45], Hamersma and Hart [46], Rouhani and Axelsson I [47] and Huq and Loth [48]). The present comparison is done for a heat flux of 5kW/m² and the simulation conditions indicated in the Table 1. The following figure illustrates the comparison results.

Table 1
Operating conditions for the simulation of two-phase flow parameters

Parameter	Value
Heat flux (kW/m²)	0.5, 2, 3, 4, 5, 10, 25
Tube diameter (mm)	25
Tube length (m)	1
Ammonia mass fraction in the inlet	0.6
Inlet pressure (bar)	13

From Fig. 1 we observe that the numerical values achieved in the present work show similar trend to the results of other models. For void fractions lower than 0.6 there is a great similarity between the calculated values using Rouhani and Axelsson's correlation and our results, being the absolute deviation between 1.6 and 8.3 %. For void fractions above 0.6, the absolute deviation is larger and can reach 10.8 %. Regarding the Zivi's model, which is applicable for annular flow regime ($\alpha > 0.8$), it gives values very close to our simulation results. The absolute deviation of this model does not exceed 5.5% and may decrease to 0.37%. The same results it obtained with Smith, Lockhart Martinelli, Hamersma and Hart correlation in the same void fraction range. However, a large error between our simulation results and those calculated from Smith, Lockhart Martinelli, Hamersma, Hart and Zivi correlations for a void fraction less the 0.75 where the deviation is more than 23% and achieve 78%.

Respecting the order of the void fraction, there is good agreement between our model and the other models.

3.2 Liquid and vapor velocities

In order to understand the influence of the heat flux on the fluctuation and the hydrodynamics of the two-phase flows in the bubble pump, the variations of the liquid and vapor velocities for different values of the heat flux for 5 and 20 seconds are plotted in Figs. 2to 6.

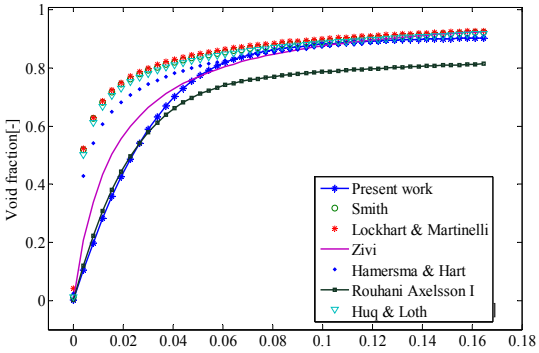

Fig. 1. Void fraction versus vapor quality

Figs. 2 and 3 show the variation of liquid and vapor velocity for a heat flux of 2kW.m^{-2}. From these figures, it can be seen that the velocities profiles are subdivided into two zones:

Zone (I): The liquid and vapor velocities increase against the time, while the fluctuation appears at the beginning and then gradually decreases until they are completely damped. The duration of fluctuation is about 12 seconds. The flow fluctuations observed are due to the weak generation of the steam; therefore the pumping action is not continuous. In this region the gravitational and frictional affects domain the pumping process.

Zone (II): The velocities increase without fluctuation. After 12 seconds, the amount of steam generated may be able to lift the lean solution in the bubble pump.

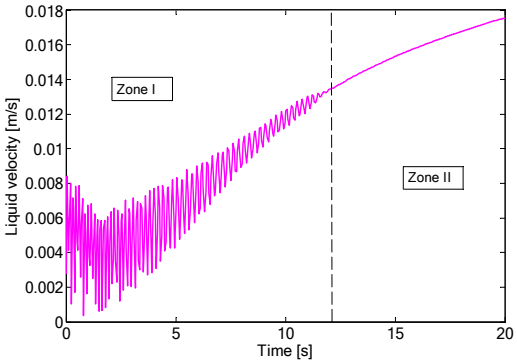

Fig. 2. Liquid velocity vs. time for q=2 kW.m^{-2}

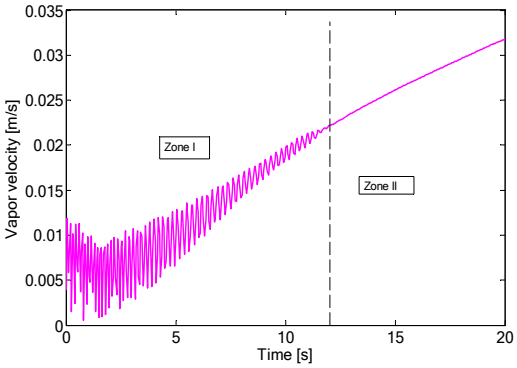

Fig. 3. Vapor velocity vs. time for q=2 kW.m^{-2}

With the purpose of comparing the liquid and vapor velocities profiles and evaluating the difference between them, their variations as a function of time are plotted on the same graph in Fig. 4 for a heat flux of 5 kW.m^{-2}. According to this figure, it can be seen that these velocities begin their evolution with a fluctuation for 6 seconds. During this period, flow in the bubble pump is dominated by the bubbly regime, where, the nucleate bubbles can't form a slug because of the condensation phenomenon. Then, we notice that the liquid velocity increases slightly to stabilize at around 0.03m/s indicating the establishment of the steady-state. However, the vapor velocity increases slightly due to the continuation of generating vapor.

The influence of the heat supplied to the bubble pump on the behavior of liquid and vapor velocities is shown in Figs. 5 and 6. For the first 4 seconds, a vigorous fluctuation is observed for the two velocities, we can't distinguish the influence of the heat input in fact of the little period of the fluctuation against the simulation time. In this period the

fluctuation amplitude is at its maximum. After that, a reduction of the fluctuation amplitude against the time is shown. In addition, the velocities curves can be distinguished against the heat input; liquid and vapor velocities increase if the heat input increase. The generate vapor increases cause an increase of vapor and liquid velocities and a reduction of fluctuation. The period of the fluctuation is reduced too by the increase of the heat input.

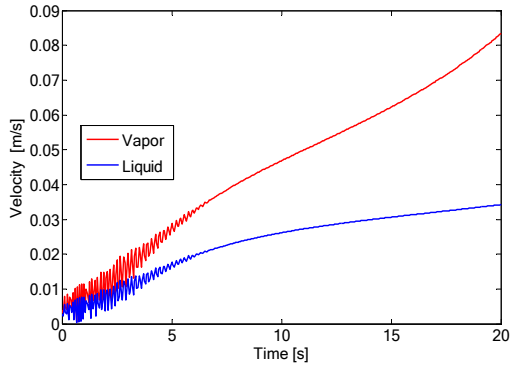

Fig. 4. Liquid and vapor velocities vs. time for q=5 kW.m^{-2}

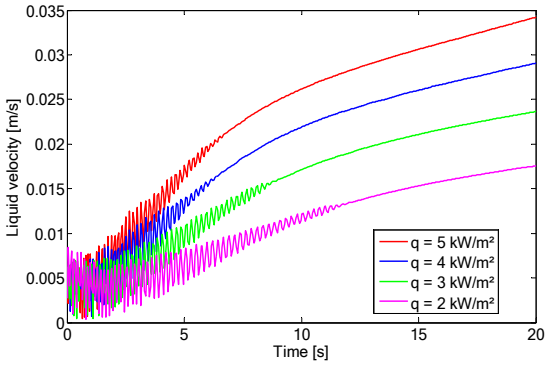

Fig. 5. Liquid velocity against time for different heat input.

We noticed in Table 2 the fluctuation duration for liquid and vapor velocities in the function of heat input to the bubble pump. By examining the values in Table 2, we remark, for these velocities, the same fluctuation duration for each heat flux study. The indicated duration decreases with the increase of heat input. The fluctuation is continuing along with 12s for the lower heat flux studied. Then it becomes constant until 4kW/m² of a heat flux value.

Table 2

Duration of velocities fluctuations for different heat fluxes

Heat flux (W/m²)	**Fluctuation duration (s)**	
	Liquid velocity	**Vapor velocity**
5	6.2	6.3
4	6.1	6.3
3	8.2	8.1
2	12	11.9

After the period of fluctuation, liquid and vapor velocities increase against time and against heat put. The absence of the fluctuation indicates that a slug regime dominates the other regimes. Liquid velocity tends to stabilize; however, vapor velocity values increase slightly for the higher heat input.

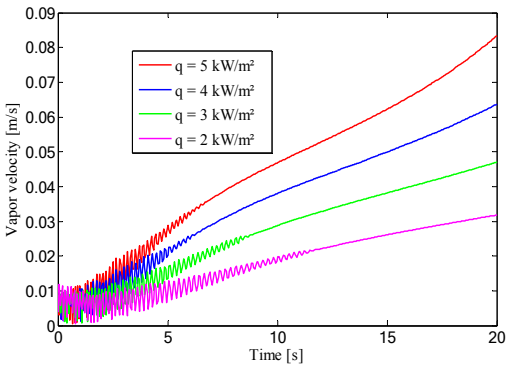

Fig. 6. Vapor velocity against time for different heat input

As it's shown if Fig. 7 mass velocity behavior takes the same shape as liquid and vapor velocities, this for the range of heat flux studied. In the beginning, it starts its evolution by a period of fluctuation. The duration of fluctuation increase from 6s to 12s for a heat flux decreases from 5 to 2kW/m². The slope of the mass velocity curve increases in function of heat flux in the fluctuation zone. After this, mass velocity makes a little period of growth before to stabilizing. Mass velocity achieves at the stabilizing state its maximum value, where it increases if the heat flux increases.

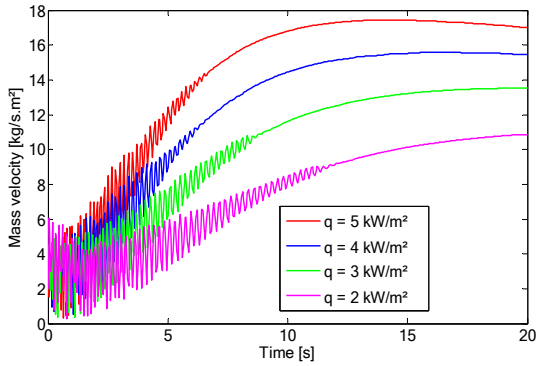

Fig. 7. Time evolution of mass velocity for different heat flux.

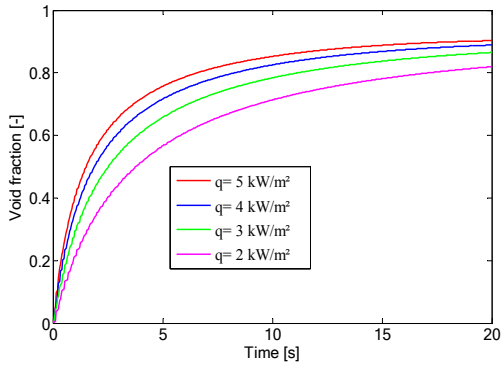

Fig. 8. Time void fraction behavior for different heat flux.

3.3 Void fraction

The void fraction is an important parameter for the two-phase flow in the bubble pump. It is used to estimate the amount of refrigerant desorbed in this element.

The variation of the void fraction over time for the different heat flux studied is shown in Fig. 8. The behavior of the void fraction is not similar to this of velocities studied. It is clear that there is no fluctuation of the void fraction over time and for the different heat flux studied. In fact, the evolution of the void fraction as a function of time is not related to the hydrodynamic condition in the pump which may be responsible for the flow fluctuation. Therefore, the void fraction is not influenced by the change in the flow regime configuration because it grows without disturbance.

The void fraction is influenced by the change in the heat flux values. From Fig. 8, it can be seen that the void fraction increases if heat flux increases too. From void fraction, it's possible to define the flow regimes versus time for the different heat flux studied. The relative time of the flow regimes is defined on the basis of the critical void fractions. The values of these fractions are 0.3, 0.5, and 0.8, which correspond to the limits of the bubbly, slug, and churn regimes respectively [30, 39]. The relative time of each regime as a function of heat flux is given in Table 3.

For the higher heat flux (q=3, 4, and 5 $kW.m^{-2}$), it can be seen that the void fraction at the outlet of the bubble pump increases and then tends to stabilize. In the range of heat flux studied, churn and annular regimes are dominant in the bubble pump tube. The churn regime lasts 40% and 28% of the total simulation time for q=3 and 4 kW/m^2 respectively. Whereas the annular regime takes 45% and 60% of total time in the bubble pump respectively for the heat indicated above. For heat flux of $2kW/m^2$, the flow regime in the bubble pump is dominated by the churn regime, where it takes 57.5% of the simulation time. On the other hand, the duration of the bubbly and slug regimes decreases as the heat flux increases.

Tableau 3

Relative duration of different flow regimes

Heat flux (W/m^2)	Relative duration of flow regime			
	Bubbly	**Slug**	**Churn**	**Annular**
0.5	31	63.42	5.5	0
1	15	31	54	0
2	7.5	15	57.5	20
3	5	10	40	45
4	3.75	7.75	28.5	60
5	3	6	22.5	68.5

3.4 Pumping action of the bubble pump

The bubble pump is the key part of an absorption-diffusion refrigeration machine since it plays a double role: it pumps the solution from the low to the high level and desorbs the refrigerant. The pumping ratio is the parameter that characterizes the pumping action in the bubble pump. The pumping ratio

represents the ratio of the liquid velocity to the vapor velocity.

The variation of the pumping rate as a function of time for different heat fluxes is shown in Fig. 9. It can be seen from Fig. 9 that the pumping ratio increases overtime for a heat flux of 2kW.m^{-2}. However, it increases, reaches a maximum, and then decreases for flux densities of 5, 10, 15, 20, and 25 kW.m^{-2}.

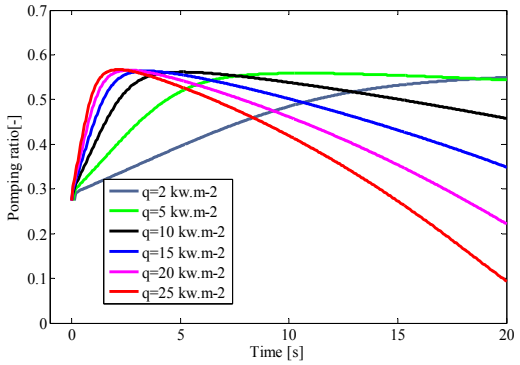

Fig. 9. Time pumping action evolution for different heat flux.

It should be noted that despite the high desorption for the heat flux of 25kW.m^{-2}, this range of heat flux does not allow the bubble pump to operate properly, given the low values of the pumping ratio at the outlet during steady-state operation. For the other heat flux, the optimal operation of the bubble pump is achieved for heat flux range between 2 to 10 kW.m^{-2}, since the pumping ratio decreases over time during steady-state operation while maintaining the higher values.

4. Conclusion

In the present work, the flow fluctuation in the thermal bubble pump of absorption-diffusion refrigerators was simulated by using a drift flow model. A mixing of ammonia-water is heated along the bubble pump tube. The influence of heat supplied of the bubble pump for a transitional regime was studied. Five hydrodynamic parameters were simulated such as liquid, vapor, and mass velocities in addition to void fraction and the pumping ratio.

Liquid, vapor, and mass velocities start their evolution versus time by a period of fluctuation. It was found that the fluctuation duration increase in averages from 6 to 12s for heat flux supplied to the bubble pump decreasing from 5 to 2kW/m². The simulated void fraction allows defining the relative time occupied by each regime. The maximum relative time for the slug regime is about 63.42% for a heat flux of 0.5kW/m². However, an increase of heat flux to 5kW/m² causes a dominance of annular flow, where the relative time is 68.5%.

From the simulation of the pumping ratio, it's recommended to apply a heat flux of less than 10kW/m² to reach the desired pumping action of the bubble pump.

Appendix 1: Tiliner-Roth and Friend correlation [41]

The density of the liquid solution is calculated as for a quasi-ideal solution for the equation:

$$\rho_m = x_m = x\rho_{NH_3,T^*_{NH_3}} + (1-x)\rho_{H_2O,T^*_{H_2O}} + \Delta\rho_{Tsol,x}$$

Where the « excess » density in relation to the ideal solution is approximated with the function:

$$\Delta\rho_{T^{\therefore}_{sol},x} = \left[x(1-x) - Ax^2(1-x)\right]\rho^{0.5}_{NH_3,T^*_{NH_3}}\rho^{0.5}_{H_2O,T^*_{H_2O}}$$

The parameter A is a function of the temperature of the solution such that :

$$A = \sum_{i=0}^{2} A_{1,i}T^{\therefore i}_{sol} + \frac{\sum_{i=0}^{2} A_{2,i}T^{\therefore i}_{sol}}{x}$$

$$T^{\therefore}_{sol} = \frac{T_{sol}}{T_{c,H_2O}}$$

The parameters A1 and A2 are as follows:

	i = 0	**i = 1**	**i = 2**
A_1	-2.410	8.310	-6.924
A_2	2.118	-4.050	4.443

The calculation of the density using these correlations is valid for temperatures between 0°C and 250°C.
The density of the pure substance is calculated from the equation :

$$\frac{\rho_L}{\rho_c} = \sum_{i=0}^{6} A_i \tau^{b_i}$$

	H_2O		NH_3	
i	**A**	**b**	**A**	**b**
0	1.0	0	1.0	0
1	1.9937718430	1/3	2.02491283	1/3
2	1.0985211604	2/3	0.84049667	2/3
3	-0.509449299	5/3	0.30155852	5/3
4	-1.761912427	16/3	-0.20926619	16/3
5	-44.90054802	43/3	-74.6025017	43/3
6	-723692.2618	110/3	4089.792775	70/3

Appendix 2: Pátek and Klomfar correlation [42]

$$H_L(T,x) = H_0 \sum_i a_i \left(\frac{T}{T_0} - 1\right)^{m_i} x^{n_i}$$

H_0 = 100 kJ.kg^{-1}andT_0 = 273.16 K

i	m_i	n_i	a_i
1	0	1	-7.61080
2	0	4	25.6905
3	0	8	-247.092
4	0	9	325.952
5	0	12	-158.854
6	0	14	61.9084
7	1	0	11.4314
8	1	1	1.18157
9	2	1	2.84179
10	3	3	7.41609
11	5	3	891.844
12	5	4	-1613.09
13	5	5	622.106
14	6	2	-207.588
15	6	4	-6.87393
16	8	0	3.50716

References

[1] A. Benhmidene, B. Chaouachi, S. Gabsi, A review of bubble pump technologies, J. Applied Science 10 (2011) 1806–1813.

[2] M. Ledinegg, Instability of flow during natural and forced circulation, Die Wärme 61 (1938) 891–898.

[3] R. Yang J. Feng and H. Lin, The analysis of density wave instability in a boiling flow system, 2nd Int. Symp. Multiphase Flow and Heat Transfer1 (Sian, China, 1989).

[4] H.C. Unal, Density-Wave Oscillations in Sodium Heated Once-Through Steam Generator Tubes, J. Heat Transfer 103 (1981) 485-496.

[5] R. C. Torok, T. C. Derbidge and J. M. Healzer, Water level measurement uncertainty during BWR instability, Nucl. Eng. and Design 151(1994) 173-184.

[6] B. I. Nigmatulin O. I. Melikhov, V. N. Blinkov and P. G. Gakal, The numerical analysis of boiling flow instability in parallel heated channels, Nucl. Eng. and Design139 (1993) 235-1243.

[7] G. Yadigaroglu, Two-phase flow instabilities and propagation phenomena, Thermohydraulics of two-phase systems for industrial design and nuclear engineering, McGraw-Hill 2 19-34,1981.

[8] J. Bouré and A. Mihaila, The oscillatory behaviour of heated channels, EUROATOM, Symposium of two-phase flow dynamics, Eindhoven 695–720, 1967.

[9] J. Maulbetsch and P. Griffith, A study of system-induced instabilities in forced convection flows with subcooled boiling, MITengineering projects Lab Report 5382-35, 1965.

[10] N. Zuber and J.A. Findlay, Average volumetric concentration in two-phase flow systems, J. Heat Transfer 87 (1965) 453-486.

[11] A. Stenning and T. Veziroglu, Flow oscillation modes in forced convection boil, Heat Transfer Fluid Mech. Stanford Univ, Press 301–316, 1965.

[12] K. Fukuda and T. Kobor, Classification of two-phase flow instability by density wave oscillation model, J. Nuclear Technology 16 (1979) 95–108.

[13] F. Mayinger, Status of thermohydraulic research in nuclear safety and new challenges, Eight International Topical Meeting on Nuclear Reactor Thermal-Hydraulics 1508–1518, 1997.

[14] A.Z. Fatimah MohdSaat and Artur J. Jaworski, The Effect of Temperature Field on Low Amplitude Oscillatory Flow within a Parallel-Plate Heat Exchanger in a Standing Wave

Thermoacoustic System, App. Sciences 7 (2017) 417.

[15] B.Sailaja, G. Srinivas, B. Suresh Babu, Free and Forced Convective Heat Transfer through a Nanofluid with Two Dimensions past Stretching Vertical Plate, Int. J. Thermofluid Science and Technology 7(3) (2020) 070302.

[16] A.Benhmidene K.S. Arjun B. Chaouachi, CFD parametric investigation for two-phase flow of ammonia-water mixing in bubble pump tube, Thermal Sciences 25 (2021) 433-448.

[17] R. Jemai A. Benhmidene K. Hidouri and B. Chaouachi, Simulation of Ammonia-Water Two Phase Flow in Bubble Pump, Int. J. Mech. and Mechatronics Engineering 11 (2017) 1473 - 1477.

[18] A. Benhmidene B. Chaouachi S. Gabsi and M. Bourouis, Experimental investigation on the flow behaviour in a bubble pump of diffusion absorption refrigeration systems,Case Studies in Thermal Engineering 8 (2016) 1-9.

[19] S. Mazouz R. Mansouri and A. Bellagi, Experimental and thermodynamic investigation of an ammonia/water diffusion absorption machine, Int. J. refrigeration 4 (2014) 464–470.

[20] Y. Belkassmi, L. Elmaimouni1, A. Rafiki, K. Gueraoui, N. Hassanain, Heat and mass transfer modeling during laminar condensation of non-cryogenic downward fluids flow in a small vertical tube, Int. J. Thermofluid Science and Technology 7(2020) 070401.

[21] Y. Zhou, L. Zhang, S. Bu, C. Sun , W. Xu , Y. Xiao, L. Liu, Study on Heat Transfer Characteristics of the Whole Plate Fin Tube Cooler, Int. J. Thermofluid Science and Technology 7(2) (2020) 070204.

[22] R. Jemaii A. Benhmidene and B. Chaouachi, Influence of the tube diameter on instability in the bubble pump, International Conference on Green Energy Conversion Systems (GECS)Hammamet (2017) 1-5.

[23] R. Garma Y. Stiriba M. Bourouis and A. Bellagi, Numerical investigations of the heating distribution effect on the boiling flow in bubble pumps, Int. J. of Hydrogen Energy, 39 (2014) 15256-15260.

[24] C. S. Brooks B. Ozar T. Hibiki and M. Ishii, Two-group drift-flux model in boiling flow, Int. J. Heat and Mass Transfer 55 (2012) 6121-6129.

[25] A. Benhmidene B. Chaouachi S. Gabsi and M. Bourouis, Modelling of Boiling Two-phase Flow in the Bubble Pump of Diffusion-Absorption Refrigeration Cycles, Chem. Engineering. Communications 202 (2015) 15-24.

[26] A. Benhmiden and B. Chaouachi, Investigation of pressure drops in the bubble pump of absorption-diffusion cycles, App. Thermal Engineering 161 (2019) 114101.

[27] A. Benhmidene B. Chaouachi M. Bourouis and S. Gabsi, Numerical prediction of flow patterns in the bubble pump, J. Fluid Engineering ASME, 133 (2011) 031302-0313.

[28] D. E. Turney D. V. Kalaga M. Ansari R. Yakobovand J. B. Joshi. Reform of the Drift Flux Model of Multiphase Flow in Pipes, Wellbores, and Reactor Vessels. Chem. Engineering. Science 184 (2018) 251-258.

[29] H. Goda T. Hibiki S. Kim M. Ishii and J. Uhle, Drift-flux model for downward two-phase flow, Int. J. Heat and Mass Transfer 46 (2003) 4835-4844.

[30] N. Zuber, J.A, Findlay Average volumetric concentration in two-phase flow systems. Journal of Heat Transfer, 87 (1965) 453-468.

[31] T. Hibiki and M. Ishii,One-dimensional drift–flux model for two-phase flow in a large diameter pipe,Int. J Heat and Mass Transfer 46 (2003) 1773–1790.

[32] T. Hibiki and M. Ishii,One-dimensional drift-flux model and constitutive equations for relative motion between phases in various two-phase flow regimes, Int. J. Heat and Mass Transfer46 (2003) 4935–4948.

[33] M. Ishii. One-dimensional drift-flux model and constitutive equations for relative motion between phases in

various two-phase flow regimes (ANL--77-47).United States, (1977).

[34] W. M. Rohsenow J. P. Hartnett and E.N. Ganic, Handbook of heat transfer fundamentals, New-York: McGraw-Hill Book Company (1985).

[35] J. R. Thome. Wolverine Heat Transfer Engineering Data book III, Decatur: Wolverine Tube, Inc (2010).

[36] A. Benhmidene B. Chaouachi S. Gabsi and M. Bourouis. Modelling of the heat flux received by a bubble pump of absorption-diffusion refrigeration cycles, Heat Mass Transfer 47 (2011) 1341–1347.

[37] A. Hainoun E. Hicke and J. Wolters.Modelling of void formation in the subcooled boiling regime in the ATHLET code to simulate flow instability for research reactors, Nucl. Eng. and Design 16 (1996) 7175-7191.

[38] P. G.Rousseau,Thermal-fluid systems modelling II, Potchefstroom: North-West University (2010).

[39] A. Benhmidene B. Chaouachi S. Gabsi and M. Bourouis.Effect of operating conditions on the performance of the bubble pump of absorption-diffusion refrigeration cycles. Thermal Sciences 15 (2011) 793-806.

[40] P. Bourseau and R. Bugarel. Absorption-Diffusion Machines: Comparison of the Performances of NH_3 –H_2O and NH_3 – NaSCN, Int. J. Refrigeration 9 (1986) 206–214.

[41] R. Tillner-Roth, and D. G. Friend. Survey and assessment of available measurements on thermodynamic proprieties of the mixture (ammonia + water), J. of physical chemical references 27 (1998) 45-61.

[42] J. Pátek, and J. Klomfar.Simple Functions for Fast Calculations of Selected Thermodynamic Properties of Ammonia–Water system, Int. J. Refrigeration 18 (1995) 228–234.

[43] S. L .Smith, Void fractions in two phase flow: a correlation based upon an equal velocity head model,Proc. Inst. Mech. Engrs 84 (1969) 647–657.

[44] R. W. Lockhart, R. C. Martinelli, Proposed correlation of data for isothermal two-phase, two component flow in pipes», Chem. Eng. Progress 45 (1949) 39–48.

[45] S. M. Zivi, Estimation of steady state steam void fraction by means of the principle of minimum entropy production, Trans. ASME, J. Heat Transfer 86 (1964) 247–252.

[46] P. J. Hamersma, J. Hart, A pressure drop correlation for gas/liquid pipe flow with a small liquid holdup, Chem. Eng. Sciences 42 (1987) 1187–1196.

[47] S. Z. Rouhani, E.Axelsson, Calculation of void volume fraction in the sub cooled and quality boiling regions, Int. J. Heat Mass Transfer 13 (1970) 383–393.

[48] R. H. Huq, J. L. Loth, Analytical two phase flow void fraction prediction method, J. Thermo Physic 6 (1992)139–144.